

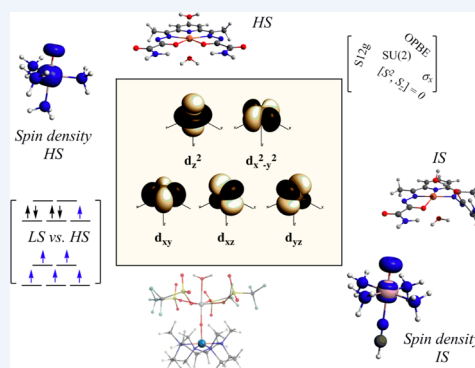
## Spinning around in Transition-Metal Chemistry

Marcel Swart\*<sup>†,‡,§</sup> and Maja Gruden<sup>§</sup><sup>†</sup>ICREA, Pg. Lluís Companys 23, 08010 Barcelona, Spain<sup>‡</sup>Institut de Química Computacional i Catàlisi (IQCC) & Dept. Química, Universitat de Girona, Campus Montilivi, 17071 Girona, Spain<sup>§</sup>Center for Computational Chemistry and Bioinformatics, Faculty of Chemistry, University of Belgrade, Belgrade 11000, Serbia

**CONSPECTUS:** The great diversity and richness of transition metal chemistry, such as the features of an open d-shell, opened a way to numerous areas of scientific research and technological applications. Depending on the nature of the metal and its environment, there are often several energetically accessible spin states, and the progress in accurate theoretical treatment of this complicated phenomenon is presented in this Account.

The spin state energetics of a transition metal complex can be predicted theoretically on the basis of density functional theory (DFT) or wave function based methodology, where DFT has advantages since it can be applied routinely to medium-to-large-sized molecules and spin-state consistent density functionals are now available. Additional factors such as the effect of the basis set, thermochemical contributions, solvation, relativity, and dispersion, have been investigated by many researchers, but challenges in unambiguous assignment of spin states still remain. The first DFT studies showed intrinsic spin-state preferences of hybrid functionals for high spin and early generalized gradient approximation functionals for low spin. Progress in the development of density functional approximations (DFAs) then led to a class of specially designed DFAs, such as OPBE, SSB-D, and S12g, and brought a very intriguing and fascinating observation that the spin states of transition metals and the  $S_N2$  barriers of organic molecules are somehow intimately linked.

Among the many noteworthy results that emerged from the search for the appropriate description of the complicated spin state preferences in transition metals, we mainly focused on the examination of the connection between the spin state and the structures or coordination modes of the transition metal complexes. Changes in spin states normally lead only to changes in the metal–ligand bond lengths, but to the best of our knowledge, the dapsox ligand showed the first example of a transition-metal complex where a change in spin state leads also to changes in the coordination, switching between pentagonal-bipyramidal and capped-octahedron. Moreover, we have summarized the results of the thorough study that corrected the experimental assignment of the nature of the recently synthesized  $Sc^{3+}$  adduct of  $[Fe^{IV}(O)(TMC)]^{2+}$  (TMC = 1,4,8,11-tetramethylcyclam) and firmly established that the  $Sc^{3+}$ -capped iron–oxygen complex corresponds to high-spin  $Fe^{III}$ . Last, but not least, we have provided deeper insight and rationalization of the observation that unlike in metalloenzymes, where the  $Fe^{IV}$ -oxo is usually observed with high spin, biomimetic  $Fe^{IV}$ -oxo complexes typically have a intermediate spin state. Energy decomposition analyses on the trigonal-bipyramidal (TBP) and octahedral model systems with ammonia ligands have revealed that the interaction energy of the prepared metal ion in the intermediate spin state is much smaller for the TBP structure. This sheds light on the origin of the intermediate spin state of the biomimetic TBP  $Fe^{IV}$ -oxo complexes.



## 1. INTRODUCTION

The chemistry of the first-row transition metals is highly diverse with a multitude of different reactivity and property patterns. This richness results from a wide range of ligands and flexibility of coordination around the metal, but most of all it results from the partial occupation of the shell of d-orbitals, which leads to different oxidation and spin states. Metal oxidation states (used as chemically intuitive labels<sup>1</sup>) are quite well understood and controllable, although exceptions occur,<sup>2,3</sup> but the spin states remain an enigmatic aspect of increasing interest, as exemplified in the first text-book devoted entirely to it.<sup>4</sup> Spin, postulated for the first time by Uhlenbeck and Goudsmit,<sup>5</sup> is a fundamental property of all elementary particles. In transition-metal complexes, the electronic spin can manifest itself as unpaired

electrons at the metal; however, there also exist redox noninnocent ligands that make the situation more complex by taking on unpaired electrons. Moreover, depending on the oxidation state of the metal, and the coordination sphere, several spin states might be energetically accessible. Of course, having a different number of unpaired electrons has a direct effect on the structure, magnetism, and reactivity of molecules.

Insights into spin states of transition-metal complexes can be obtained from synthesis, spectroscopy, or computational studies and in some cases from catalysis (based on the arguments from above). However, the assignment of spin states

Received: May 31, 2016

Published: November 14, 2016

and the role it plays in, for example, reactivity is not unambiguous. The combination of a variety of techniques therefore is needed, which has led to the formation of a European collaborative network (COST Action CM1305). The focus of this network is on metalloenzymes, spin-crossover compounds, and biomimetic complexes. Several research groups present in the network have already shown the advantages of combining synthesis, spectroscopy and theory: K. Meyer and co-workers<sup>6</sup> used spectroscopy (X-ray, Mössbauer, and EPR) and quantum chemistry to study the synthesis, structure, and reactivity of a d<sup>3</sup> iron(V) nitride complex; DeBeer, Neese and co-workers<sup>7</sup> used a combination of X-ray emission spectroscopy and quantum chemistry to study the nature of the “long-overlooked” atom in the FeMo-cofactor of nitrogenase; F. Meyer and co-workers<sup>8</sup> reported on the unusual spectroscopy of a tetracarbene oxoiron(IV) complex with exceedingly high separation between the  $S = 1$  and  $S = 2$  states with spectroscopy (X-ray and Mössbauer) and quantum chemistry; finally, Duboc and co-workers<sup>9</sup> reported on a nickel-centered H<sup>+</sup> reduction catalyst that models multiple states of the [NiFe]-hydrogenase enzyme using electrochemical and spectroscopic (EPR, Mössbauer, IR, and UV–vis) techniques combined with quantum chemistry.

In this Account, we focus exclusively on our computational studies, to show how theory is becoming ever more powerful and increasingly plays a more important role in these collaborative studies. We start with the origin of the problems more than a decade ago, address how this was approached by us, and show recent successes.

## 2. A HISTORICAL SKETCH OF THEORY AND SPIN STATES

Ever since the immense progress of density functional approximations (DFAs) started in the 1990s, an increasing amount of computational studies use a variety of DFAs for transition-metal chemistry (see also Cramer and Truhlar<sup>10</sup>). Solomon and co-workers favored a spectroscopically calibrated method (BP86 with 10% Hartree–Fock (HF) exchange),<sup>11</sup> while others argued for adaptation of the amount of HF exchange in hybrid functionals (i.e., Reiher’s<sup>12</sup> B3LYP\* or the B3LYP\*\* variant<sup>13</sup> of it). The main problem with DFAs for spin states was probably first noted in 2001, when Trautwein and co-workers<sup>14</sup> reported on spin-crossover compounds and showed that none of the standard DFAs available at that time was able to describe well the spin-crossover (SCO) phenomenon (simultaneously, this led Reiher to develop his B3LYP\* functional<sup>12,15</sup>). In SCO, a low-spin state is found at low temperatures and at a certain point (the transition temperature) suddenly a switch is made to the high-spin state due to a cooperative effect. Trautwein showed that standard generalized gradient approximation (GGA) DFAs favored low-spin states, while hybrid functionals including HF exchange favored high-spin states. In other words, none of those methods was able to describe the existence of the switching process from the low to the high-spin state. That was the situation when we started to work in the field of spin-state chemistry in 2003.

Early in 2001, Handy and Cohen reported a new exchange functional (OPTX),<sup>16</sup> which showed the best coherence with HF exchange energies for atoms (deviation of only ca. 3 kcal·mol<sup>-1</sup>), and showed promising behavior for organic chemistry.<sup>17</sup> Intrigued by this, we explored its use as well for spin states of iron complexes, by combining it with a variety of correlation functionals. Fortunately, the combination with the

PBEC correlation functional<sup>18</sup> gave excellent results, and hence a new density functional approximation was born (OPBE).<sup>19</sup> In line with Perdew’s approach to use a fixed amount of HF exchange (25%),<sup>20</sup> also the corresponding hybrid (OPBE0) was tested<sup>21</sup> and quickly discarded because of the problems for hybrid functionals: the more HF exchange one puts in, the more one stabilizes the high-spin states. This is easily understood<sup>22</sup> since Hartree–Fock always favors high spin states: in HF there is no electron correlation between unlike spins ( $\alpha\beta$ ), only exchange between like spins ( $\alpha\alpha$  or  $\beta\beta$ ), and hence the more (favorable) exchange interactions there are, the more stable is the system. High spin states have more unpaired (parallel) electrons and hence more exchange interactions. This is also the origin for the exchange-enhanced reactivity (EER) model by Shaik and co-workers.<sup>23</sup>

Wave function methods on the other hand can also be applied to transition-metal complexes but require experience as they cannot be applied in a black-box fashion.<sup>24</sup> In 2006, Pierloot and co-workers reported<sup>25</sup> multiconfigurational CASPT2 results for three iron(II) complexes. One of us explored the use of DFAs<sup>26</sup> and found, not surprisingly, that OPBE gives excellent results that are on top of the CASPT2 data. More recently, Gagliardi and co-workers<sup>27</sup> corroborated this for metal–organic frameworks where they used OPBE for the larger system after having validated its robustness for the smaller building block by comparison with CASPT2. Also coupled cluster (CCSD(T)) and multireference configuration interaction (MR-CI) can be used, but these methods come at great computational expense.<sup>28</sup> Most recently, the density matrix renormalization group (DMRG)<sup>29</sup> has been put forward as an efficient method to include more orbitals in the multiconfigurational wave function, and multiconfiguration pair-density functional theory (MC-PDFT)<sup>30</sup> was proposed as a promising mix of DFT and MC methods.

An important aspect for both DFAs and wave function methods is the basis set used. The Slater-type orbital (STO) basis sets used in the ADF program<sup>31</sup> were shown to be converging very rapidly.<sup>32</sup> In contrast, Gaussian-type orbital (GTO) basis sets converged much slower, and extensive GTO basis sets were needed<sup>32</sup> to reach the same spin-state splittings as obtained with STOs. One of the most important aspects of the GTOs was the use of only two d-functions for the metal, which was already shown by Hay<sup>33</sup> in 1977 to be insufficient: at least three d-functions are needed.<sup>34,35</sup> Another widely used approach is to combine an effective core potential (ECP), a model Hamiltonian for the core electrons of the metal, with a valence basis (B). The most popular of these ECPBs (LANL2DZ, LACVP, etc.) give systematically different spin-state splittings than those obtained with STO/GTO basis sets.<sup>32</sup> Only with the more recent cc-pVTZ-pp ECPB does the result come close again.<sup>36</sup>

A recent review by Kepp<sup>37</sup> further reported some other effects within computational chemistry (zero-point enthalpy, entropy, free energy, solvation, relativity, dispersion energy) on the spin state splittings. Finally, it should be mentioned that often hybrid functionals lead to spin-contamination, and there exist methods for doing the spin-decontamination automatically (including for gradients and frequencies within the QUILD program<sup>35,38</sup>).

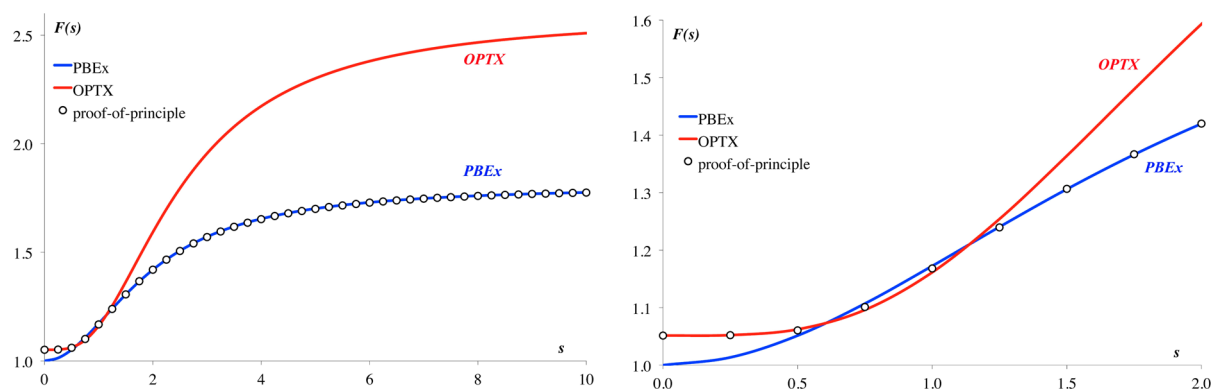


**Figure 1.** Exchange enhancement factor,  $F(s)$  for PBEx and OPTX, overall (left) and low  $s$  region (right).

### 3. A SURPRISING CONNECTION BETWEEN BIMOLECULAR $S_N2$ REACTIONS AND SPIN STATES

Intrigued by the good performance of OPBE for spin states and  $S_N2$  reaction barriers<sup>39</sup> and the failure for weak interactions,<sup>40,41</sup> every aspect of the difference between OPBE and PBE was explored. This is because these two functionals showed opposite behavior: OPBE works well for spin states and  $S_N2$  barriers (PBE not) but fails for weak interactions (PBE does work well). The only difference is in the exchange energy (OPTX vs PBEx); hence that part determines these differences. The shape of the exchange enhancement factor  $F(s)$  is completely different (see equations below and Figure 1) and therefore first the low  $s$  limit ( $s$  is a dimensionless density gradient) and the large  $s$  (Lieb–Oxford) region were explored,<sup>42</sup> but without any success.

$$E^{\text{exchange}} = \int d^3 r \epsilon_x^{\text{unif}}(\rho) F(s); \quad s = \frac{|\nabla \rho|}{2\rho k_F}$$

$$k_F = [3\pi^2 \rho]^{1/3}$$

$$F(s)^{\text{OPTX}} = A + B \frac{(Cs^2)^2}{(1 + Cs^2)^2}$$

$$F(s)^{\text{PBEx}} = D + Es^2 \frac{1}{1 + (E/F)s^2} = D + F \frac{1}{1 + (F/E)s^{-2}}$$

$$F(s)^{\text{proof-of-principle}} = G + \frac{Hs^2}{1 + Js^2} - \frac{Ks^2}{1 + Ls^4}$$

$$A = 1.05151, B = 1.538582, C = 0.364624, D = 1.0,$$

$$E \approx 0.219515, F = 0.804, G = A, H = 0.191458,$$

$$J = \frac{H}{1 + F - A}, K = 0.180708, E = 4.036674$$

The breakthrough came<sup>43</sup> with a switching function to explore which region of the exchange enhancement function was responsible for the different results observed. In this switch experiment, up to a point  $s = P - 0.1$  the OPTX formula was used, after  $s = P + 0.1$  the PBEx formula, and a smooth interpolation was used around  $P$  to go smoothly from OPTX to PBEx;  $P$  was varied from 0.1 au to 20.0 au in steps of 0.1 au (as shown by the white spheres in Figure 2). The outcome was crystal clear<sup>43</sup> (see Figure 2): both the spin states and  $S_N2$  barriers are completely determined by the  $F(s)$  region between  $s = 0$  and  $s = 1$ , it is irrelevant whether one uses the OPTX formula or PBEx for values larger than  $s = 1$ . At the same

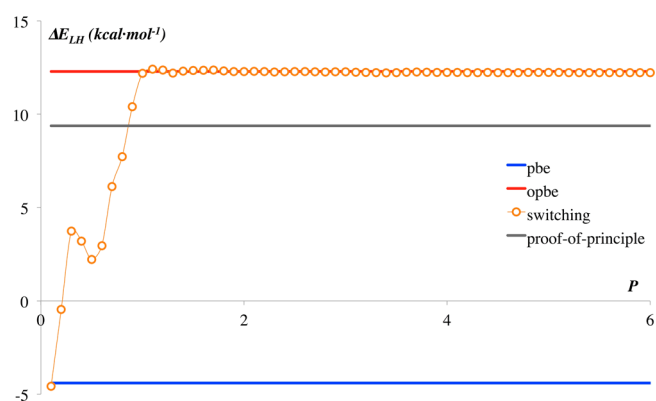


**Figure 2.** Spin-state splitting by switching from PBE to OPBE (see text).

time,<sup>43</sup> the weak interactions are almost completely insensitive to the region of  $s < 1$ . This immediately opened up a new route for the design of a pure density functional that could be accurate for both spin states,  $S_N2$  barriers, and weak interactions. Instead of switching through interpolation, a mathematical formulation was constructed (see “proof-of-principle” above) that followed as closely as possible OPTX up to ca.  $s = 0.7$  and PBEx from ca.  $s = 1.0$  (see Figure 1).<sup>43</sup> This proof-of-principle DFA<sup>43</sup> indeed performed as expected with results for spin states (see Figure 2) and  $S_N2$  barriers close to those of OPBE, and weak interactions close to those of PBE. After adding Grimme’s ( $D_2$ ) dispersion energy,<sup>44</sup> also the  $\pi$ – $\pi$  stacking energies were very good, and subsequently the six parameters in the new DFA were optimized against 10 reference sets where either high-level computational data (CCSD(T) with large basis sets) or experimental data were available. This led to the SSB-D functional in 2009<sup>45</sup> and, after refinement to make it numerically more stable and including Grimme’s  $D_3$  dispersion energy,<sup>46</sup> to the S12g functional.<sup>47</sup> Specific examples of application of these DFAs to transition-metal complexes can be found in our recent book chapter.<sup>48</sup>

A number of observations should be added: none of the SSB-D and S12g functionals, nor other ones that are popular for chemistry (B97-D<sub>3</sub>,<sup>44,46</sup> B3LYP-D<sub>2</sub>, OPBE, etc.), satisfy the uniform-gas limit, that is, the exchange enhancement factor  $F(s)$  does not go to 1 at  $s = 0$  but to a value between 1.038 and 1.087 (depending on the functional). This is significant for heterogeneous catalysis, for example, because for solid state physics LDA is a very good functional, and any deviation from the uniform-gas limit will severely hinder the application to

these systems. Second, unlike the situation with Grimme dispersion<sup>46</sup> for other DFAs, within the design of SSB-D and S12g, the  $D_2/D_3$  parameters are optimized simultaneously with the other parameters.

One of the most important conclusions of these studies is however that the spin states of transition metals and the  $S_{N2}$  barriers of organic molecules are somehow intimately linked. Our studies showed that pure DFAs that significantly improve upon standard pure functionals (e.g., LDA, BP86, BLYP, PBE, TPSS) for reaction barriers will work well for spin states. For instance, for  $S_{N2}$  barriers, standard GGA functionals give a mean absolute deviation (MAD) compared to high-level theory of ca. 6–7 kcal·mol<sup>-1</sup>.<sup>39</sup> OPBE, SSB-D, and S12g instead show a MAD value of 2.6–3.4 kcal·mol<sup>-1</sup>.<sup>45,47</sup> Simultaneously, for two iron(II) complexes, one low-spin ( $S = 0$ ) with pyridines as axial ligands and the other high-spin ( $S = 2$ ) with chlorides as axial ligands, all three (OPBE, SSB-D, and S12g) correctly describe the spin state for both complexes.<sup>47</sup> In fact, out of a total of more than 50 DFAs, only eight (among which the three mentioned above) were able to do so.<sup>47</sup>

The prediction of the close connection between  $S_{N2}$  barriers and spin states was put to the test when Perdew and co-workers reported last year the “made very simple” (MVS) and “strongly constrained and appropriately normed” (SCAN)<sup>49</sup> meta-GGA functionals.<sup>50</sup> Unlike SCAN,<sup>50</sup> MVS drastically improved the performance for barriers: for a reference set with 76 barrier heights standard (meta-)GGA functionals (and SCAN) gave MAD values of 8–11 kcal·mol<sup>-1</sup>; MVS reduces the MAD to 4.6 kcal·mol<sup>-1</sup>.<sup>50</sup> Moreover, unlike SCAN,<sup>50</sup> for the two iron complexes MVS is able to correctly predict the spin state,<sup>51</sup> the first time this happens for any of the nonempirical DFAs by Perdew and co-workers. Most interestingly, MVS satisfies the uniform-gas limit (by design), so MVS might be considered the first DFA that is equally accurate in chemistry and in physics.<sup>51</sup>

#### 4. GROUND AND EXCITED STATES OF TRANSITION METAL COMPLEXES

In the past decade, we and others have investigated a variety of transition-metal complexes (Mn, Fe, Co, Ni, Cu) for spin state properties. We looked at metallocenes and the corresponding molecular cages,<sup>22,52</sup> spin-crossover complexes and whether their cooperative behavior might be predicted by focusing on single transition-metal complexes,<sup>53</sup> the effect of spin-crossover in solution,<sup>54</sup> how subtle (spin) effects control polymerization reactions,<sup>55</sup> and how the coordination sphere around a transition-metal may be different for different spin states of the same transition-metal complex.<sup>56</sup> This latter case is quite common for coordination spheres around a metal in different oxidation states, with, for example, a preferred tetrahedral coordination around copper(I) vs an octahedral/square planar coordination around copper(II). For one and the same complex, changes in spin states may show longer metal–ligand distances (due to occupation of antibonding orbitals in higher spin states), but usually no difference in coordination is observed. Surprisingly, for the *dapsox* ligand with a total of 11 potential ligand atoms (see Figure 3), we observed<sup>56</sup> pentagonal bipyramidal (PBPY-7), capped octahedron (OCF-7), capped trigonal prism (TPRS-7), and square-pyramidal (SPY-5) coordination modes. Although the ground state corresponded in most cases to PBPY-7 (both experimentally and computationally), the other spin states were found to favor different coordination modes. To the best of our knowledge

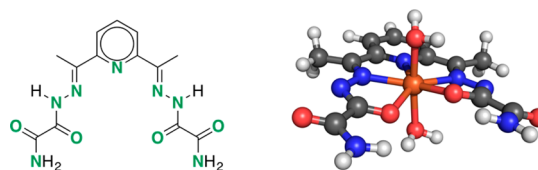


**Figure 3.** 2,6-Diacetylpyridinebis(semioxamamide) ( $H_2dapsox$ ) ligand (left) and geometry of most stable coordination mode<sup>56</sup> (right).

this was the first time that such spin-state coordination-mode chemistry was observed.

#### 5. METAL-OXO COMPLEXES AND LEWIS ACIDS

High-valent transition-metal complexes are involved in the activation of small molecules, giving, for example, metal-oxo or metal-nitrene species.<sup>57–59</sup> Different oxidation states can be observed for these different species, for example, ranging from III to V for iron. We recently investigated the molecular structure and spectroscopic properties for a total of 16 iron(III)-oxo, iron(III)-hydroxo, iron(III)-peroxo, iron(III)-hydroperoxo, and iron(IV)-oxo species.<sup>2,60</sup> Excellent results were obtained for Fe–O and Fe–N distances with mean absolute deviations on the order of 0.01–0.02 Å by using PBE-D<sub>2</sub>/TZ2P. It should be noted that in ref 2 two outliers were reported,  $[Fe^{III}(OH)(H_3buea)]^-$  ( $H_3buea = 1,1,1$ -tris[ $(N'$ -tert-butylureaylato)- $N$ -ethyl]aminato) and  $[Fe^{III}(OOH)(TMC^i)]^{2+}$ , that showed apparent deviations of ca. 0.08–0.10 Å. However, upon reinvestigating the original sources,<sup>61,62</sup> it was found that the experimental data mentioned in ref 2 were referring to complexes with iron in a different oxidation state; the actual experimental Fe–O distances for  $[Fe^{III}(OH)(H_3buea)]^-$  (1.93 Å)<sup>61</sup> and  $[Fe^{III}(OOH)(TMC^i)]^{2+}$  (1.85 Å)<sup>62</sup> are in fact in excellent agreement with the computed data of 1.95 and 1.84 Å, respectively. In a follow-up paper,<sup>60</sup> we showed that by using the BP86-D<sub>3</sub>/TDZP method we could achieve the same or better accuracy in a much faster way.

The biomimetic  $Fe^{IV}$ -oxo complexes typically have an  $S = 1$  intermediate spin state. This is in contrast to metalloenzymes where the  $Fe^{IV}$ -oxo is usually observed with  $S = 2$  high spin. Exceptions exist such as with the  $H_3buea$ , 1,1,1-tris(2-[N2-(1,1,3,3-tetramethylguanidino)]ethyl)amine (TMG<sub>3</sub>tren), or tris(5-phenylpyrrol-2-ylmethyl)amine (tpa<sup>ph</sup>) ligands, which all have trigonal coordination around the  $Fe^{IV}$  and show  $S = 2$  high-spin states. Most of the other biomimetic  $Fe^{IV}$ -oxo complexes, such as with the TMC ligand, instead have a tetragonal coordination around  $Fe^{IV}$ . In order to enhance our understanding of the connection between spin states and ligand, we explored how well we can reproduce these features with simple model systems of  $[(NH_3)_nFe^{IV}(O)(Y)]^{2+}$ . Model systems have been used before, for example, by Shaik<sup>63</sup> or Baerends,<sup>64</sup> but they focused more on reactivity. A number of different views on the importance of spin states for reactivity is present in the literature, with among others the two-state (or exchange-enhanced) reactivity by Shaik and co-workers,<sup>23,65</sup> the frontier molecular orbitals by Baerends and co-workers who focus on low-lying acceptor orbitals,<sup>64,66</sup> and the driving force argument by Saouma and Mayer based on the Hammett postulate.<sup>67</sup> Interestingly enough, the best performing DFA compared to CCSD(T) barriers was found to be our OPBE.<sup>63</sup>

The model systems allowed us to use fully symmetric  $C_{3v}$  ( $n = 3$ ,  $Y = NH_3$  or MeCN) and  $C_{4v}$  ( $n = 4$ ,  $Y = MeCN$ ) coordination around the iron. Similar to what was observed

experimentally and computationally, the  $C_{3v}$  systems have a high-spin  $S = 2$  ground state, and the  $C_{4v}$  systems an intermediate  $S = 1$  ground state. Also the spin-state splittings ( $\Delta E_{\text{HI}} = \Delta E_{\text{H}(S=2)} - \Delta E_{\text{I}(S=1)}$ ;  $C_{3v}$   $-17.7 \text{ kcal}\cdot\text{mol}^{-1}$ ,  $C_{4v}$   $+7.8 \text{ kcal}\cdot\text{mol}^{-1}$ ) were similar to the values observed for the  $\text{H}_3\text{buea}$  ( $C_{3v}$   $-16.2 \text{ kcal}\cdot\text{mol}^{-1}$ ) or TMC ( $C_{4v}$   $+5.0 \text{ kcal}\cdot\text{mol}^{-1}$ )  $\text{Fe}^{\text{IV}}$ -oxo complexes, for example. We could rationalize this by using an energy decomposition analysis similar to what we did before.<sup>22,68</sup> The  $[\text{Fe}^{\text{IV}}(\text{O})]^{2+}$  unit on its own has a high-spin  $S = 2$  state, and in order to attain an  $S = 1$  state after complexation with a ligand, it first needs to be prepared (excited) to an  $S = 1$  spin state, corresponding to the valence excitation energy ( $\Delta E_{\text{valexc}}$ ) and deformation energy. Subsequently the prepared  $[\text{Fe}^{\text{IV}}(\text{O})]^{2+}$  fragment can interact with the ligand, leading to a favorable interaction energy. The results are shown in Figure 4,

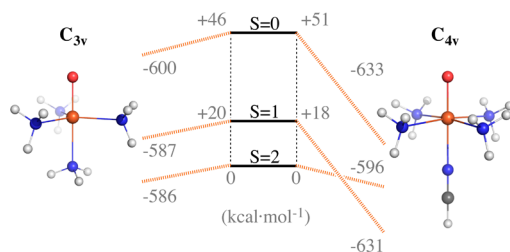


**Figure 4.** Energy decomposition analysis for binding of  $[\text{Fe}^{\text{IV}}(\text{O})]^{2+}$  unit with  $C_{3v}$  and  $C_{4v}$  symmetric ligands.

which shows clearly the origin for going from a preferred  $S = 1$  state in  $C_{4v}$  symmetry to a preferred  $S = 2$  state in  $C_{3v}$  symmetry. The preparation energy needed to bring the  $[\text{Fe}^{\text{IV}}(\text{O})]^{2+}$  unit from its preferred  $S = 2$  state to an  $S = 1$  state is on the order of  $20 \text{ kcal}\cdot\text{mol}^{-1}$ . For the  $C_{4v}$  symmetric ligands, this is largely overcome by the more favorable interaction energy of the  $S = 1$  state with the ligands, which at  $-631 \text{ kcal}\cdot\text{mol}^{-1}$  is ca.  $35 \text{ kcal}\cdot\text{mol}^{-1}$  more favorable than the  $-596 \text{ kcal}\cdot\text{mol}^{-1}$  for the  $S = 2$  state. Although the interaction energy of the  $S = 0$  state is even slightly better than that for the  $S = 1$  state, the preparation energy is too unfavorable for it to be competitive.

The picture changes completely when we look at the  $C_{3v}$  symmetric ligands: the interaction energy is smaller for all three spin states, but most dramatically so for the  $S = 1$  state where it is almost  $45 \text{ kcal}\cdot\text{mol}^{-1}$  smaller. More importantly, it is now

equal to the interaction energy of the  $S = 2$  state with the  $C_{3v}$  ligand. Since there is still the preparation energy of ca.  $20 \text{ kcal}\cdot\text{mol}^{-1}$  for the  $[\text{Fe}^{\text{IV}}(\text{O})]^{2+}$  unit, the  $S = 2$  has now become the spin ground-state. An in-depth analysis of the binding of the  $[\text{Fe}^{\text{X}}(\text{O})]^q$  unit with the molecular orbitals of the ligands and the role of spin states on it will be reported elsewhere.<sup>69</sup>

Apart from the geometric data, we also calculated<sup>2</sup> Mössbauer parameters for the 16 complexes and found in general very good agreement with experimental data. The isomer shift ( $\delta$ ) was typically found to agree with experiment within  $0.01\text{--}0.05 \text{ mm}\cdot\text{s}^{-1}$ , except for the iron complexes with the  $\text{H}_3\text{buea}$  and the  $N,N$ -bis(2-pyridylmethyl)- $N$ -bis(2-pyridyl)methylamine (N4Py) ligand, with somewhat larger differences (up to  $0.13 \text{ mm}\cdot\text{s}^{-1}$ ). The quadrupole splitting differed more, typically of the order of  $0.1\text{--}0.6 \text{ mm}\cdot\text{s}^{-1}$ . Nevertheless, in general the Mössbauer parameters could be reproduced sufficiently well so that a prediction could be made<sup>2</sup> for the effect of Lewis acids on the Mössbauer parameters of iron–oxygen species.

A few years ago, Nam and Fukuzumi reported a new iron–oxygen species, in which the  $\text{Fe}\text{--}\text{O}$  unit was capped by a  $\text{Sc}^{3+}$  moiety (see Figure 5). The addition of scandium triflate ( $\text{Sc}(\text{OTf})_3$ ) in solution to  $[\text{Fe}^{\text{IV}}(\text{O})(\text{TMC})(\text{NCCH}_3)]^{2+}$  showed interesting chemistry: without the presence of scandium triflate only one-electron reduction took place, but with  $\text{Sc}(\text{OTf})_3$  present suddenly two-electron reduction was observed. They also were able to obtain a crystal structure that showed a number of unexpected features: (i) the scandium took up a fourth triflate and additionally a fifth axial ligand, (ii) iron lost acetonitrile as its sixth ligand, and (iii) the methyl groups of the TMC ligand switched from *anti* to *syn* toward the iron–oxygen. We started working on it because no spin state was determined for the complex, and here our density functional studies might help.

There are two possible scenarios for the  $\text{Sc}^{3+}$ -capped iron–oxygen species, which might retain its IV oxidation state on iron or it could be reduced to the III state. This is directly related to the unknown axial ligand to scandium (*vide supra*) that could either be a hydroxyl (with  $\text{Fe}^{\text{IV}}$ ) or water (with  $\text{Fe}^{\text{III}}$ ). Since X-ray spectroscopy is unable to detect hydrogens, the crystal structure could coincide with either one of these possibilities. Therefore, we investigated all possible spin states (low, intermediate, high) for both oxidation states of iron. It became immediately clear<sup>2</sup> that the crystal structure corre-

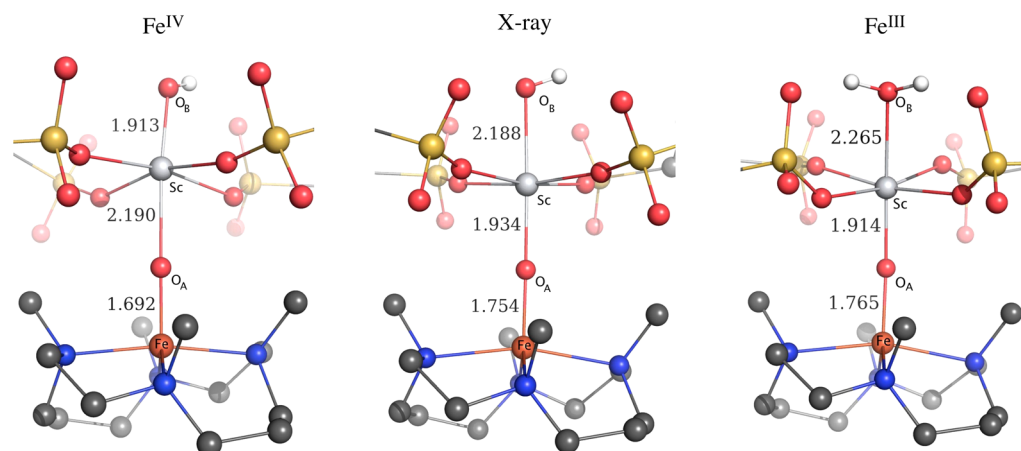


**Figure 5.** Computed  $\text{Fe}^{\text{IV}}$  and  $\text{Fe}^{\text{III}}$  structures<sup>2</sup> in comparison with X-ray structure<sup>70</sup>

sponds to high-spin Fe<sup>III</sup>. This was based on three observations: (i) the Sc–O<sub>A</sub> and Sc–O<sub>B</sub> distances (see Figure 5) were found to be respectively long–short (Fe<sup>IV</sup>), short–long (Fe<sup>III</sup>), short–long (X-ray); (ii) the Fe–O<sub>A</sub> distance is too short (Fe<sup>IV</sup>) or matches perfectly (Fe<sup>III</sup>); (iii) there is only one spin state (high-spin Fe<sup>III</sup>) out of the six that has long Fe–N distances (2.18 Å).

The application of Mössbauer spectroscopy on this delicate species was not possible at that time; hence we predicted the Mössbauer parameters for all six possible spin states. Fortunately, last year, Que, Münck, and co-workers<sup>3</sup> were able to synthesize a similar Sc<sup>3+</sup>-capped iron–oxygen species, where the axial ligand to scandium was replaced by an acetonitrile. All spectroscopic features were similar to those of the 2010 compound, and moreover now also EPR and Mössbauer spectroscopy could be performed. The observed experimental Mössbauer parameters showed excellent agreement with the computational predictions: the isomer shift of  $\delta = 0.36(3) \text{ mm}\cdot\text{s}^{-1}$  and quadrupole splitting  $\Delta E_Q = -1.02(5) \text{ mm}\cdot\text{s}^{-1}$  are on top of the computed values of  $0.39 \text{ mm}\cdot\text{s}^{-1}$  and  $-0.99 \text{ mm}\cdot\text{s}^{-1}$ , respectively. Hence, it was firmly established that the Sc<sup>3+</sup>-capped iron–oxygen complex corresponds to high-spin Fe<sup>III</sup>, which was furthermore confirmed in a similar Cr(III)-capped Fe<sup>III</sup>–oxygen complex.<sup>71</sup>

## 6. CONCLUDING REMARKS

Spin states of transition-metal complexes are essential for understanding many cases in biology, medicine, catalysis, and photonics. The choice of theoretical method, basis set, solvation and many other effects represent factors that need to be considered to be able to deal with the close-lying spin states in coordination compounds. However, the assignment of spin states is not unambiguous. A combination of synthesis, theoretical simulations, and crystallographic and spectroscopic characterization has to be used to tackle the problems at hand, which has led to enrichment of our understanding of transition-metal chemistry and new approaches such as Shaik's exchange-enhanced reactivity, Baerends' low-lying acceptor orbitals, or Mayer's driving force. In seeking to develop appropriate DFAs for the treatment of spin states and weak interactions, it became clear that there is an intriguing link between the spin states of transition metals and S<sub>N</sub>2 barriers of organic molecules.

Our work has uncovered multiple examples of the influence of the spin state on the coordination environment of a transition metal. It demonstrated the possibility to question the experimentally predicted spin and oxidation states and give rationalization for the nature of the spin state preferences in important biomimetic species. Most importantly, through detailed studies on these systems we have begun to develop and provide key insights into the subtle interplay between the complicated electronic structure and the structural, mechanistic, and spectroscopic observables.

## AUTHOR INFORMATION

### Corresponding Author

\*Marcel Swart. E-mail: [marcel.swart@icrea.cat](mailto:marcel.swart@icrea.cat).

### ORCID

Marcel Swart: 0000-0002-8174-8488

### Author Contributions

The manuscript was written through contributions of all authors. All authors have given approval to the final version of the manuscript.

## Funding

The following organizations are thanked for financial support: MINECO (projects CTQ2014-59212-P and CTQ2015-70851-ERC), GenCat (project 2014SGR1202 and XRQTC), European Fund for Regional Development (FEDER, UNGI10-4E-801), and Serbian Ministry of Science. This work was performed in the framework of the COST action CM1305 "Explicit Control Over Spin-states in Technology and Biochemistry (ECOSTBio)".

## Notes

The authors declare no competing financial interest.

## Biographies

**Marcel Swart** obtained his Ph.D. in Chemistry from the University of Groningen and is currently ICREA Research Professor and director of the IQCC institute at the University of Girona, and Chair of COST Action CM1305. He is developing computational research tools and applying these in studies on (bio)inorganic chemistry with a special emphasis on spin states.

**Maja Gruden** obtained her Ph.D. in Chemistry from the University of Belgrade and is currently Associate Professor at Faculty of Chemistry-University of Belgrade. Her main research interest is accurate computing of ground and excited state properties of transition metal complexes by DFT and development and extension of multireference DFT techniques for simulations in systems where electron degeneracy or near-degeneracy requires the use of multideterminantal approaches.

## REFERENCES

- (1) Hoffmann, R.; Alvarez, S.; Mealli, C.; Falceto, A.; Cahill, T. J.; Zeng, T.; Manca, G. From Widely Accepted Concepts in Coordination Chemistry to Inverted Ligand Fields. *Chem. Rev.* **2016**, *116*, 8173–8192.
- (2) Swart, M. A change in oxidation state of iron: scandium is not innocent. *Chem. Commun.* **2013**, *49*, 6650–6652.
- (3) Prakash, J.; Rohde, G. T.; Meier, K. K.; Jasniowski, A. J.; Van Heuvelen, K. M.; Münck, E.; Que, L., Jr. Spectroscopic Identification of an Fe<sup>III</sup> Center, not Fe<sup>IV</sup>, in the Crystalline Sc–O–Fe Adduct Derived from [Fe<sup>IV</sup>(O)(TMC)]<sup>2+</sup>. *J. Am. Chem. Soc.* **2015**, *137*, 3478–3481.
- (4) *Spin States in Biochemistry and Inorganic Chemistry: Influence on Structure and Reactivity*; Swart, M., Costas, M., Eds.; Wiley: Oxford, 2015.
- (5) Uhlenbeck, G. E.; Goudsmit, S. Ersetzung der Hypothese vom unmechanischen Zwang durch eine Forderung bezüglich des inneren Verhaltens jedes einzelnen Elektrons. *Naturwissenschaften* **1925**, *13*, 953–954.
- (6) Scepianiak, J. J.; Vogel, C. S.; Khusniyarov, M. M.; Heinemann, F. W.; Meyer, K.; Smith, J. M. Synthesis, Structure, and Reactivity of an Iron(V) Nitride. *Science* **2011**, *331*, 1049–1052.
- (7) Lancaster, K. M.; Roemelt, M.; Ettenhuber, P.; Hu, Y.; Ribbe, M. W.; Neese, F.; Bergmann, U.; DeBeer, S. X-ray Emission Spectroscopy Evidences a Central Carbon in the Nitrogenase Iron-Molybdenum Cofactor. *Science* **2011**, *334*, 974–977.
- (8) Meyer, S.; Klawitter, I.; Demeshko, S.; Bill, E.; Meyer, F. A Tetracarbene–Oxoiron(IV) Complex. *Angew. Chem., Int. Ed.* **2013**, *52*, 901–905.
- (9) Brazzolotto, D.; Gennari, M.; Queyriaux, N.; Simmons, T. R.; Pécaut, J.; Demeshko, S.; Meyer, F.; Orio, M.; Artero, V.; Duboc, C. Nickel centred H<sup>+</sup> reduction catalysis in a model of [NiFe]-Hydrogenase. *Nat. Chem.* **2016**, *8*, 1054.
- (10) Cramer, C. J.; Truhlar, D. G. Density functional theory for transition metals and transition metal chemistry. *Phys. Chem. Chem. Phys.* **2009**, *11*, 10757–10816.

- (11) Szilagy, R. K.; Metz, M.; Solomon, E. I. Spectroscopic Calibration of Modern Density Functional Methods Using  $[\text{CuCl}_4]^{2-}$ . *J. Phys. Chem. A* **2002**, *106*, 2994–3007.
- (12) Reiher, M.; Salomon, O.; Hess, B. A. Reparameterization of hybrid functionals based on energy differences of states of different multiplicity. *Theor. Chem. Acc.* **2001**, *107*, 48–55.
- (13) Harvey, J. N.; Aschi, M. Modelling spin-forbidden reactions: recombination of carbon monoxide with iron tetracarbonyl. *Faraday Discuss.* **2003**, *124*, 129–143.
- (14) Paulsen, H.; Duelund, L.; Winkler, H.; Toftlund, H.; Trautwein, A. X. Free Energy of Spin-Crossover Complexes Calculated with Density Functional Methods. *Inorg. Chem.* **2001**, *40*, 2201–2203.
- (15) Reiher, M. Theoretical Study of the  $\text{Fe}(\text{phen})_2(\text{NCS})_2$  Spin-Crossover Complex with Reparametrized Density Functionals. *Inorg. Chem.* **2002**, *41*, 6928–6935.
- (16) Handy, N. C.; Cohen, A. J. Left-right correlation energy. *Mol. Phys.* **2001**, *99*, 403–412.
- (17) Baker, J.; Pulay, P. Assessment of the OLYP and O3LYP density functionals for first-row transition metals. *J. Comput. Chem.* **2003**, *24*, 1184–1191.
- (18) Perdew, J. P.; Burke, K.; Ernzerhof, M. Generalized Gradient Approximations Made Simple. *Phys. Rev. Lett.* **1996**, *77*, 3865–3868.
- (19) Swart, M.; Ehlers, A. W.; Lammertsma, K. Performance of the OPBE exchange-correlation functional. *Mol. Phys.* **2004**, *102*, 2467–2474.
- (20) Perdew, J. P.; Ernzerhof, M.; Burke, K. Rationale for mixing exact exchange with density functional approximations. *J. Chem. Phys.* **1996**, *105*, 9982–9985.
- (21) Swart, M.; Groenhof, A. R.; Ehlers, A. W.; Lammertsma, K. Validation of exchange-correlation functionals for spin states of iron complexes. *J. Phys. Chem. A* **2004**, *108*, 5479–5483.
- (22) Swart, M. Metal-ligand bonding in metallocenes: Differentiation between spin state, electrostatic and covalent bonding. *Inorg. Chim. Acta* **2007**, *360*, 179–189.
- (23) Shaik, S.; Chen, H.; Janardanan, D. Exchange-enhanced reactivity in bond activation by metal-oxo enzymes and synthetic reagents. *Nat. Chem.* **2011**, *3*, 19–27.
- (24) Sousa, C.; de Graaf, C. Ab Initio Wavefunction Approaches to Spin States. In *Spin States in Biochemistry and Inorganic Chemistry: Influence on Structure and Reactivity*; Swart, M., Costas, M., Eds.; Wiley: Oxford, 2015; pp 35–57.
- (25) Pierloot, K.; Vancoillie, S. Relative energy of the high- $(^5T_{2g})$  and low- $(^1A_{1g})$  spin states of  $[\text{Fe}(\text{H}_2\text{O})_6]^{2+}$ ,  $[\text{Fe}(\text{NH}_3)_6]^{2+}$ , and  $[\text{Fe}(\text{bpy})_3]^{2+}$ : CASPT2 versus density functional theory. *J. Chem. Phys.* **2006**, *125*, 124303.
- (26) Swart, M. Accurate spin-state energies for iron complexes. *J. Chem. Theory Comput.* **2008**, *4*, 2057–2066.
- (27) Isley, W. C., III; Zarrar, S.; Carlson, R. K.; Bilbeisi, R. A.; Ronson, T. K.; Nitschke, J. R.; Gagliardi, L.; Cramer, C. J. Predicting paramagnetic  $^1\text{H}$  NMR chemical shifts and state-energy separations in spin-crossover host-guest systems. *Phys. Chem. Chem. Phys.* **2014**, *16*, 10620–10628.
- (28) Rokob, T. A.; Chalupský, J.; Bím, D.; Andrikopoulos, P. C.; Srnc, M.; Rulišek, L. Mono- and binuclear non-heme iron chemistry from a theoretical perspective. *JBIC, J. Biol. Inorg. Chem.* **2016**, *21*, 619–644.
- (29) Marti, K. H.; Reiher, M. The Density Matrix Renormalization Group Algorithm in Quantum Chemistry. *Z. Phys. Chem.* **2010**, *224*, 583–599.
- (30) Li Manni, G.; Carlson, R. K.; Luo, S.; Ma, D.; Olsen, J.; Truhlar, D. G.; Gagliardi, L. Multiconfiguration Pair-Density Functional Theory. *J. Chem. Theory Comput.* **2014**, *10*, 3669–3680.
- (31) te Velde, G.; Bickelhaupt, F. M.; Baerends, E. J.; Fonseca Guerra, C.; van Gisbergen, S. J. A.; Snijders, J. G.; Ziegler, T. Chemistry with ADF. *J. Comput. Chem.* **2001**, *22*, 931–967.
- (32) Güell, M.; Luis, J. M.; Solà, M.; Swart, M. Importance of the basis set for the spin-state energetics of iron complexes. *J. Phys. Chem. A* **2008**, *112*, 6384–6391.
- (33) Hay, P. J. Gaussian basis sets for molecular calculations. The representation of 3d orbitals in transition-metal atoms. *J. Chem. Phys.* **1977**, *66*, 4377–4384.
- (34) Mitin, A. V.; Baker, J.; Pulay, P. An improved 6-31G\* basis set for first-row transition metals. *J. Chem. Phys.* **2003**, *118*, 7775–7782.
- (35) Swart, M.; Güell, M.; Luis, J. M.; Solà, M. Spin-State-Corrected Gaussian-Type Orbital Basis Sets. *J. Phys. Chem. A* **2010**, *114*, 7191–7197.
- (36) Swart, M. Spin states of (bio)inorganic systems: successes and pitfalls. *Int. J. Quantum Chem.* **2013**, *113*, 2–7.
- (37) Kepp, K. P. Consistent descriptions of metal-ligand bonds and spin-crossover in inorganic chemistry. *Coord. Chem. Rev.* **2013**, *257*, 196–209.
- (38) Swart, M.; Bickelhaupt, F. M. QUILD: QUAntum-regions interconnected by local descriptions. *J. Comput. Chem.* **2008**, *29*, 724–734.
- (39) Swart, M.; Solà, M.; Bickelhaupt, F. M. Energy landscapes of nucleophilic substitution reactions: A comparison of density functional theory and coupled cluster methods. *J. Comput. Chem.* **2007**, *28*, 1551–1560.
- (40) van der Wijst, T.; Fonseca Guerra, C.; Swart, M.; Bickelhaupt, F. M. Performance of various density functionals for the hydrogen bonds in DNA base pairs. *Chem. Phys. Lett.* **2006**, *426*, 415–421.
- (41) Swart, M.; van der Wijst, T.; Fonseca Guerra, C.; Bickelhaupt, F. M.  $\pi$ - $\pi$  Stacking tackled with Density Functional Theory. *J. Mol. Model.* **2007**, *13*, 1245–1257.
- (42) Swart, M.; Solà, M.; Bickelhaupt, F. M. Constraining optimized exchange. *Handb. Computat. Chem. Res.* **2010**, 97–125.
- (43) Swart, M.; Solà, M.; Bickelhaupt, F. M. Switching between OPTX and PBE exchange functionals. *J. Comput. Methods Sci. Eng.* **2009**, *9*, 69–77.
- (44) Grimme, S. Semiempirical GGA-type density functional constructed with a long-range dispersion correction. *J. Comput. Chem.* **2006**, *27*, 1787–1799.
- (45) Swart, M.; Solà, M.; Bickelhaupt, F. M. A new all-round DFT functional based on spin states and  $S_N2$  barriers. *J. Chem. Phys.* **2009**, *131*, 094103.
- (46) Grimme, S.; Antony, J.; Ehrlich, S.; Krieg, H. A consistent and accurate ab initio parametrization of density functional dispersion correction (DFT-D) for the 94 elements H-Pu. *J. Chem. Phys.* **2010**, *132*, 154104.
- (47) Swart, M. A new family of hybrid density functionals. *Chem. Phys. Lett.* **2013**, *580*, 166–171.
- (48) Daul, C.; Zlatar, M.; Gruden-Pavlovic, M.; Swart, M. Application of Density Functional and Density Functional Based Ligand Field Theory to Spin States. In *Spin States in Biochemistry and Inorganic Chemistry: Influence on Structure and Reactivity*; Swart, M., Costas, M., Eds.; Wiley: Oxford, 2015; pp 7–34.
- (49) Sun, J.; Ruzsinszky, A.; Perdew, J. P. Strongly Constrained and Appropriately Normed Semilocal Density Functional. *Phys. Rev. Lett.* **2015**, *115*, 036402.
- (50) Sun, J.; Perdew, J. P.; Ruzsinszky, A. Semilocal density functional obeying a strongly tightened bound for exchange. *Proc. Natl. Acad. Sci. U. S. A.* **2015**, *112*, 685–689.
- (51) Feixas, F.; Swart, M. Unpublished data, 2016.
- (52) Castro, A. C.; Johansson, M. P.; Merino, G.; Swart, M. Chemical bonding in supermolecular flowers. *Phys. Chem. Chem. Phys.* **2012**, *14*, 14905–14910.
- (53) Güell, M.; Solà, M.; Swart, M. Spin-state splittings of iron(II) complexes with trispyrazolyl ligands. *Polyhedron* **2010**, *29*, 84–93.
- (54) Swart, M.; Güell, M.; Solà, M. A multi-scale approach to spin crossover in Fe(II) compounds. *Phys. Chem. Chem. Phys.* **2011**, *13*, 10449–10456.
- (55) Johansson, M. P.; Swart, M. Subtle effects control the polymerisation mechanism in  $\alpha$ -diimine iron catalysts. *Dalton Trans.* **2011**, *40*, 8419–8428.
- (56) Stepanovic, S.; Andjelic, L.; Zlatar, M.; Andjelic, K.; Gruden-Pavlovic, M.; Swart, M. Role of Spin State and Ligand Charge in Coordination Patterns in Complexes of 2,6-Diacetylpyridinebis-

(semioxamazide) with 3d-Block Metal Ions: A Density Functional Theory Study. *Inorg. Chem.* **2013**, *52*, 13415–13423.

(57) McDonald, A. R.; Que, L., Jr. High-valent nonheme iron-oxo complexes: Synthesis, structure, and spectroscopy. *Coord. Chem. Rev.* **2013**, *257*, 414–428.

(58) Ray, K.; Pfaff, F. F.; Wang, B.; Nam, W. Status of Reactive Non-Heme Metal–Oxygen Intermediates in Chemical and Enzymatic Reactions. *J. Am. Chem. Soc.* **2014**, *136*, 13942–13958.

(59) Puri, M.; Que, L. Toward the Synthesis of More Reactive S = 2 Non-Heme Oxoiron(IV) Complexes. *Acc. Chem. Res.* **2015**, *48*, 2443–2452.

(60) Gruden, M.; Vlahovic, F. Z.; Swart, M. Unpublished data, 2016.

(61) MacBeth, C. E.; Gupta, R.; Mitchell-Koch, K. R.; Young, V. G., Jr.; Lushington, G. H.; Thompson, W. H.; Hendrich, M. P.; Borovik, A. S. Utilization of Hydrogen Bonds To Stabilize M–O(H) Units: Synthesis and Properties of Monomeric Iron and Manganese Complexes with Terminal Oxo and Hydroxo Ligands. *J. Am. Chem. Soc.* **2004**, *126*, 2556–2567.

(62) Cho, J.; Jeon, S.; Wilson, S. A.; Liu, L. V.; Kang, E. A.; Braymer, J. J.; Lim, M. H.; Hedman, B.; Hodgson, K. O.; Valentine, J. S.; Solomon, E. I.; Nam, W. Structure and reactivity of a mononuclear non-haem iron(III)–peroxo complex. *Nature* **2011**, *478*, 502–505.

(63) Chen, H.; Lai, W.; Shaik, S. Exchange-Enhanced H-Abstraction Reactivity of High-Valent Nonheme Iron(IV)-Oxo from Coupled Cluster and Density Functional Theories. *J. Phys. Chem. Lett.* **2010**, *1*, 1533–1540.

(64) Kazaryan, A.; Baerends, E. J. Ligand Field Effects and the High Spin–High Reactivity Correlation in the H Abstraction by Non-Heme Iron(IV)–Oxo Complexes: A DFT Frontier Orbital Perspective. *ACS Catal.* **2015**, *5*, 1475–1488.

(65) Usharani, D.; Wang, B.; Sharon, D. A.; Shaik, S. Principles and Prospects of Spin-States Reactivity in Chemistry and Bioinorganic Chemistry. In *Spin States in Biochemistry and Inorganic Chemistry: Influence on Structure and Reactivity*; Swart, M., Costas, M., Eds.; Wiley: Oxford, 2015; pp 131–156.

(66) Bernasconi, L.; Louwse, M.; Baerends, E. J. The Role of Equatorial and Axial Ligands in Promoting the Activity of Non-Heme Oxidation(IV) Catalysts in Alkane Hydroxylation. *Eur. J. Inorg. Chem.* **2007**, *2007*, 3023–3033.

(67) Saouma, C. T.; Mayer, J. M. Do spin state and spin density affect hydrogen atom transfer reactivity? *Chem. Sci.* **2014**, *5*, 21–31.

(68) Swart, M. Accurate Spin-State Energies for Iron Complexes. *J. Chem. Theory Comput.* **2008**, *4*, 2057–2066.

(69) D'Amore, L.; Swart, M. Unpublished data, 2016.

(70) Fukuzumi, S.; Morimoto, Y.; Kotani, H.; Naumov, P.; Lee, Y.-M.; Nam, W. Crystal structure of a metal ion-bound oxoiron(IV) complex and implications for biological electron transfer. *Nat. Chem.* **2010**, *2*, 756–759.

(71) Zhou, A.; Kleespies, S. T.; Van Heuvelen, K. M.; Que, L., Jr. Characterization of a heterobimetallic nonheme Fe(III)–O–Cr(III) species formed by O<sub>2</sub> activation. *Chem. Commun.* **2015**, *51*, 14326–14329.